WILEY | Hindawi

Research Article

X-Shaped Slotted Patch Biomedical Implantable Antenna for Wireless Communication Networks

Sarosh Ahmad [ID],[1,2] **Bilal Manzoor** [ID],[3] **Salman Naseer** [ID],[4] **Nilton Santos-Valdivia** [ID],[2] **Adnan Ghaffar** [ID],[5] **and Muhammad Inam Abbasi** [ID][6]

[1]*Department of Electrical Engineering and Technology, Government College University Faisalabad (GCUF), 38000, Pakistan*
[2]*Department of Signal Theory and Communications, Universidad Carlos III de Madrid (UC3M), 28911 Madrid, Spain*
[3]*Department of Telecom Engineering, University of Engineering and Technology (UET), 47050 Taxila, Pakistan*
[4]*Department of Information Technology, University of the Punjab Gujranwala Campus, 54000, Pakistan*
[5]*Department of Electrical and Electronic Engineering, Auckland University of Technology, 1010 Auckland, New Zealand*
[6]*Centre for Telecommunication Research & Innovation (CETRI), Faculty of Electrical and Electronic Engineering Technology (FTKEE), Universiti Teknikal Malaysia Melaka (UTeM), Melaka 76100, Malaysia*

Correspondence should be addressed to Muhammad Inam Abbasi; muhammad_inamabbasi@yahoo.com

Biomedical implantable antennas have a major role in biomedical telemetry applications. Therefore, a compact-size low-profile implantable antenna working in industrial, scientific, and medical (ISM) band at 915 MHz is presented. The presented antenna is a simple slotted patch fed with a coaxial probe of 50 Ω impedance. The patch consists of four slotted resonators printed on a flexible Roger Duroid RT5880 substrate ($\varepsilon_r = 2.2$, tan $\delta = 0.0009$) with the standard thickness of 0.254 mm. The complete volume of the designed antenna is 7 mm × 7 mm × 0.254 mm ($0.08\lambda_g \times 0.08\lambda_g \times 0.003\lambda_g$). The antenna covers the bandwidth from 800 MHz to 1 GHz (200 MHz) inside skin tissue. A good agreement between the simulation and measurements of the antenna has been obtained. Finally, the specific absorption rate (SAR) values have also been analyzed through simulations as 8.17 W/kg inside skin over 1 g of mass tissue. The proposed SAR values are less than the limit of the Federal Communications Commission (FCC). This antenna is miniaturized and an ideal applicant for applications in biomedical implants.

1. Introduction

Implantable medical devices (IMDs) are playing a significant role in enhancing the living conditions of the patients day by day. The telemetry system has given us many advantages by using an implantable antenna for the wireless communications between IMDs and external monitoring devices, and those advantages can be in terms of high data rates and long-distance communications [1, 2]. The schematic diagram of the implantable medical devices (IMDs) is presented in Figure 1. For the proposed model of the antenna, implantable medical devices (IMDs) are the key components [3]. The in-body antenna must be very thin in profile and should have very less values of SAR, and antennas should have flexibility for human care purposes [4]. Therefore, dur-

ing the design stage, the antenna must be compatible and flexible along with the human body. Human body tissues can interfere with the operating frequency which can damage the tissues; that is why the antenna should have broader bandwidth that can cover the required frequency band after being tested on human tissues [5]. The radiation properties of the antenna change rapidly due to the multiple layer structure of the human body. The human structure has skin, fat, bone, muscle, and blood tissues. These tissues have different dielectric properties which make it difficult for designing a biocompatible antenna to be utilized for the human body applications [6]. Many in-body antennas are designed for wireless communication at midradio band ranges between 402 and 405 MHz [7–11] and at ISM band ranges between 2.4 and 2.48 GHz [12–17]. A compact-
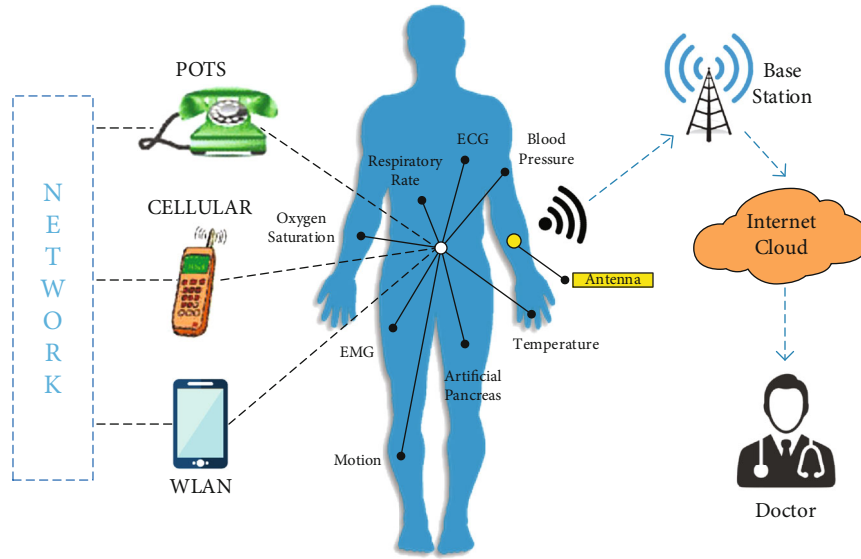
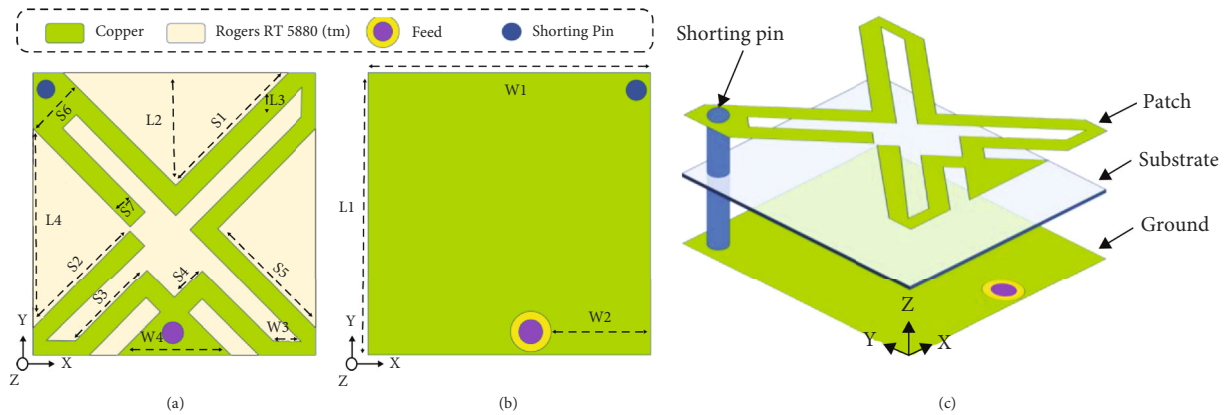FIGURE 1: Schematic diagram of the implantable medical devices (IMDs).

FIGURE 2: The proposed low-profile antenna with dimensions: (a) front view, (b) back view, and (c) exploded view.

sized broadband antenna for the implementations in biomedical implants operating at the MICS band (403 MHz) was presented in [8]. A semiflexible Roger 6010 substrate material was used with the thickness of 1.27 mm. SAR values were calculated as 284.5 W/kg over 1 g that is very high than our proposed design. Another ISM band biomedical antenna for implantable applications based on the polyimide substrate was reported in [10].

The antenna had a realized gain of -16.8 dB and the operational bandwidth of 1.22%. The complete area of the antenna was 25×20 mm^2. The realized gain and the operating bandwidth were reported as -34.9 dB and 14.9% over the reported frequency. A small-size in-body circularly polarized antenna with improved impedance matching for medical utilizations was presented in [18]. The radiating patch has circular shape, and there was an X-shaped slot inside the ground plane. The material used for the substrate was Rogers 3010 with a substrate height of 0.634 mm. Because of the two-layered substrate, the antenna profile is thick. But the antenna was less biocompatible to the human body and has high specific absorption rate (SAR) value of about

649 W/kg which is greater than the standard limit of IEEE/ IEC 6270-1 standard over 1 g of mass tissue. Another implantable antenna at 915 MHz for wireless power transfer is reported in [19]. The complete size of the antenna was $11 \times 11 \times 1.27$ mm^3, printed on a Roger 3010 substrate with an impedance bandwidth of 3.8% and the realized gain of about -29 dB. But the SAR values were not calculated, and the size of the antenna was still large with less bandwidth. An ISM band antenna for the devices in biomedical applications was reported in [20]. The antenna's size was $15 \times 15 \times 1.27$ mm^3, printed on a Roger 3010 substrate and operating at 915 MHz with the operation bandwidth of 10.6%. The antenna was being tested inside the skin, and its SAR values were found to be 517 W/kg which is a very large value than our proposed design, while another wideband implantable antenna for medical applications at the frequency of 915 MHz was proposed in [21]. The overall size of the antenna was $3.14 \times 22.09 \times 1.27$ mm^3, and the substrate material used was Roger 3010 with a thickness of 1.27 mm. The impedance bandwidth was reported as 12.2%, and the realized gain was -32.8 dB at 915 MHz. The SAR values were

TABLE 1: List of the parameters of the proposed antenna.

Parameters	Values (mm)	Parameters	Values (mm)
L1	7	S1	3.94
L2	2.79	S2	3.34
L3	0.7	S3	1.9
L4	4.8	S4	0.7
W1	7	S5	3.4
W2	3	S6	1.4
W3	0.7	S7	0.5
W4	2.7	S8	3.5

FIGURE 4: Simulation result comparison of the S_{11} for the design steps shown in Figure 3.
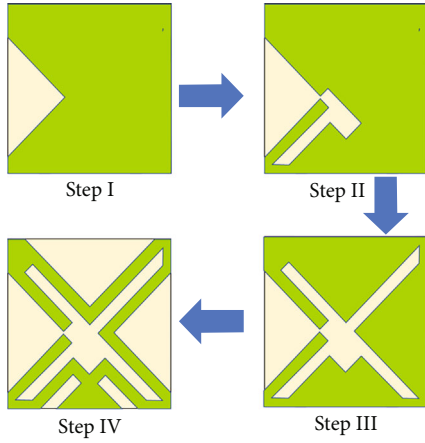

FIGURE 3: Implantable antenna design procedure: (a) truncated patch (step I), (b) slotted truncated patch (step II), (c) X-shaped slotted patch (step III), and (d) proposed design (step IV).

calculated as 778 W/kg. The antenna had large size and large SAR value as compared to our proposed design.

This article describes a compact-size implantable antenna for the biomedical applications operating in the ISM band at 915 MHz, sized at $7 \times 7 \times 0.254 \, \text{mm}^3$ $(0.08\lambda_g \times 0.08\lambda_g \times 0.003\lambda_g)$. The design employs a Rogers RT5880 substrate ($\varepsilon_r = 2.2$, $\tan \delta = 0.0009$). At 915 MHz, the antenna's radiation has an omnidirectional radiation pattern both in the E- and H-plane. The proposed design is configured with the full ground plane with four slotted resonators, so that it can provide wider bandwidth and reduced antenna back-radiation towards human skin tissue. For instance, the area of the skin is kept $20 \times 20 \, \text{mm}^2$. Because of the novel modified patch, the proposed antenna covers the more bandwidth at 915 MHz, and the peak gain of the antenna is comparable with the previous research. Fundamentally, the efficiency and designed antenna's performance under the influence of the physical body are improved, and SAR values are significantly reduced. The antenna has achieved very less SAR values and more good agreement results between simulations and measurements. This paper comprises five sections. Section 1 introduces the research work. It covers the background of the proposed research, the statement of the problem, the objectives, and the significance of the research. Section 2
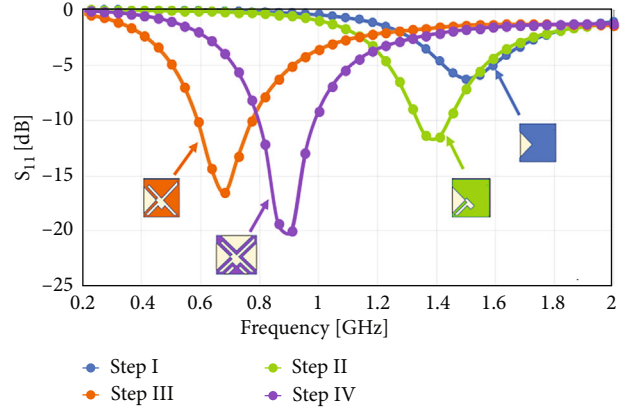

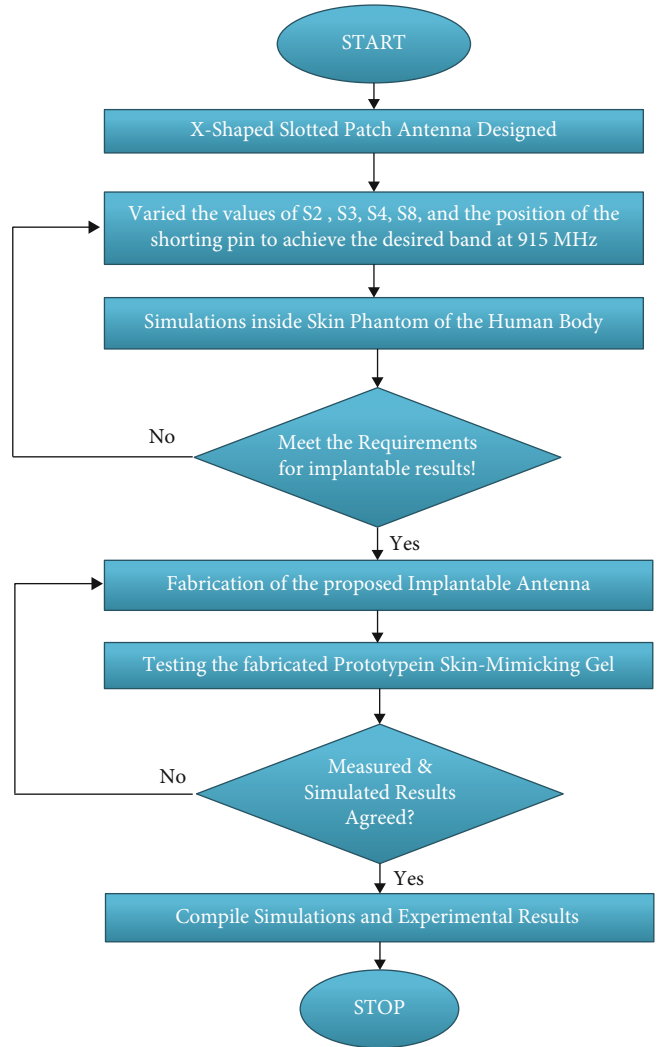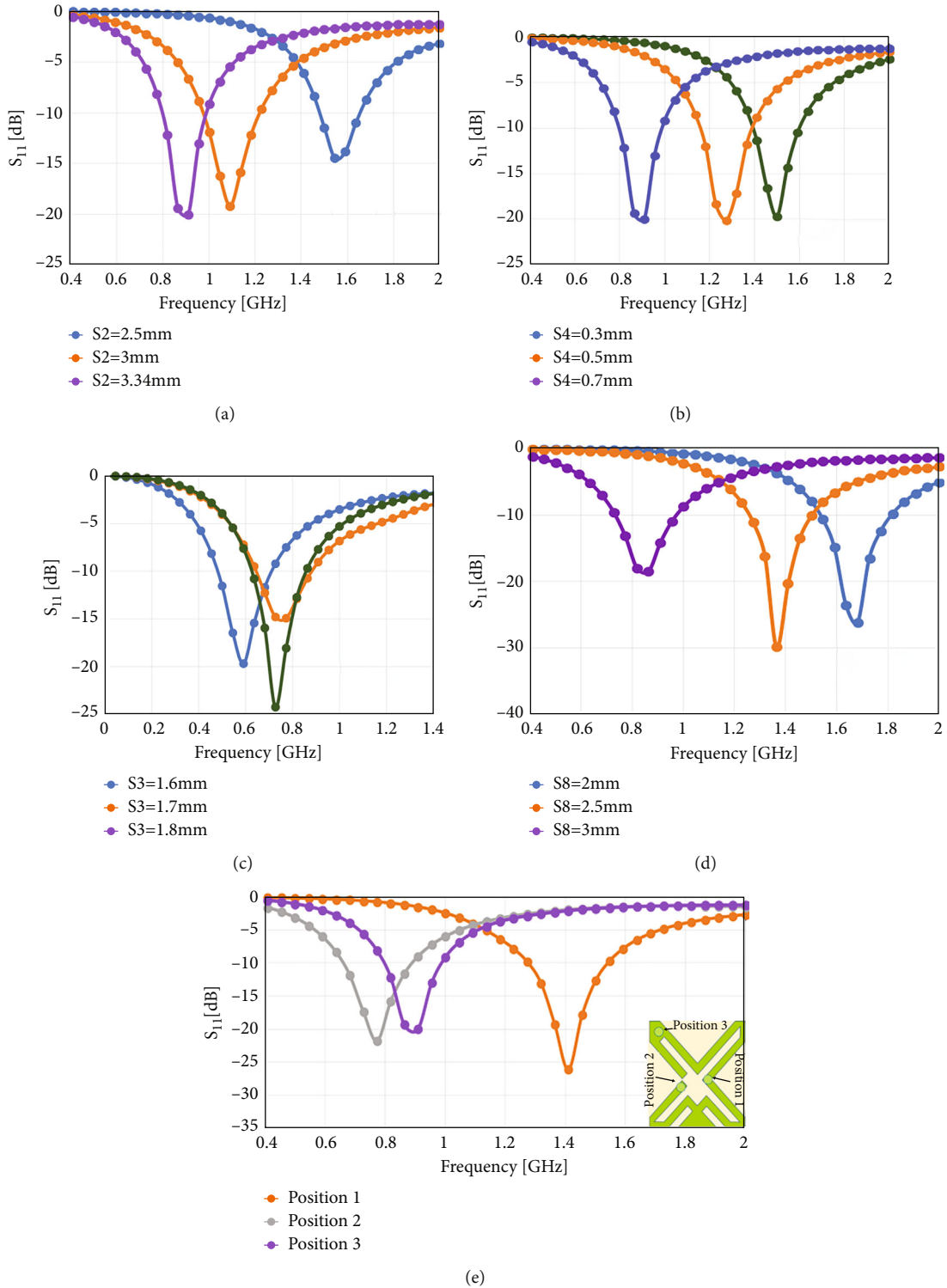FIGURE 5: Design and optimization procedure of the proposed antenna.

FIGURE 6: Parametric study of the antenna: (a) variation in "S_2"; (b) variation in "S_4"; (c) variation in "S_3"; (d) variation in "S_8"; (e) changing the position of the via.

covers the design analysis of the proposed antenna. Section 3 highlights the fabrication and measurement result and describes the antenna testing inside the skin, and Section 4 describes the conclusion.

2. Proposed Antenna Design Analysis

A slotted compact-size patch antenna with a novel-shaped radiator is fed with a coaxial probe. The presented antenna
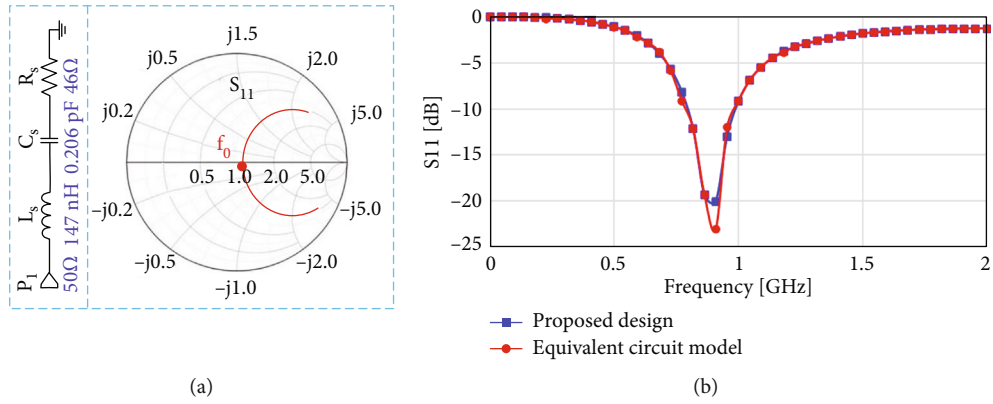
(a)   (b)

FIGURE 7: (a) Circuit modeling and the impedance matching Smith chart. (b) Comparison of the S_{11} of the proposed antenna and the equivalent circuit model.
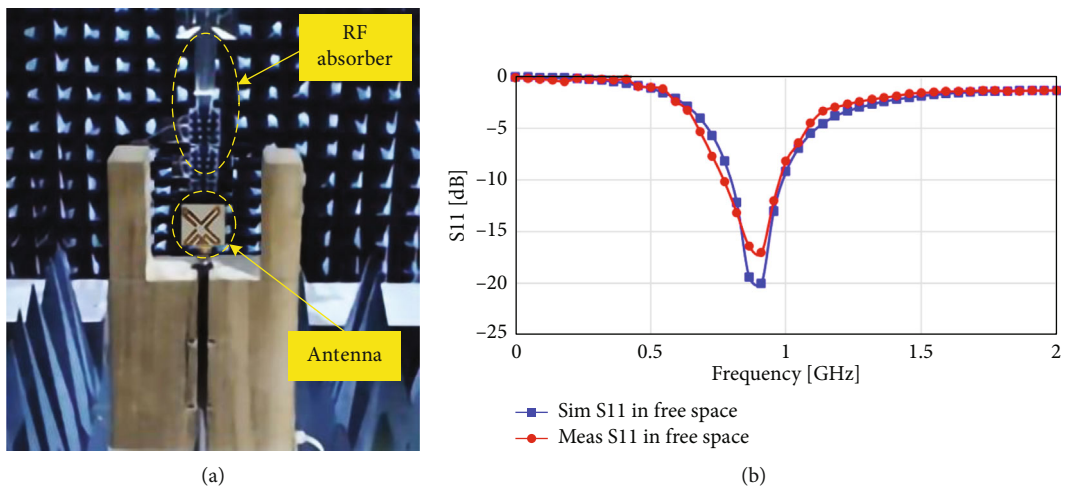

(a)   (b)

FIGURE 8: (a) Measurement setup inside chamber. (b) Comparison of the simulation and measurement reflection coefficients (dB) of the patch antenna in free space.
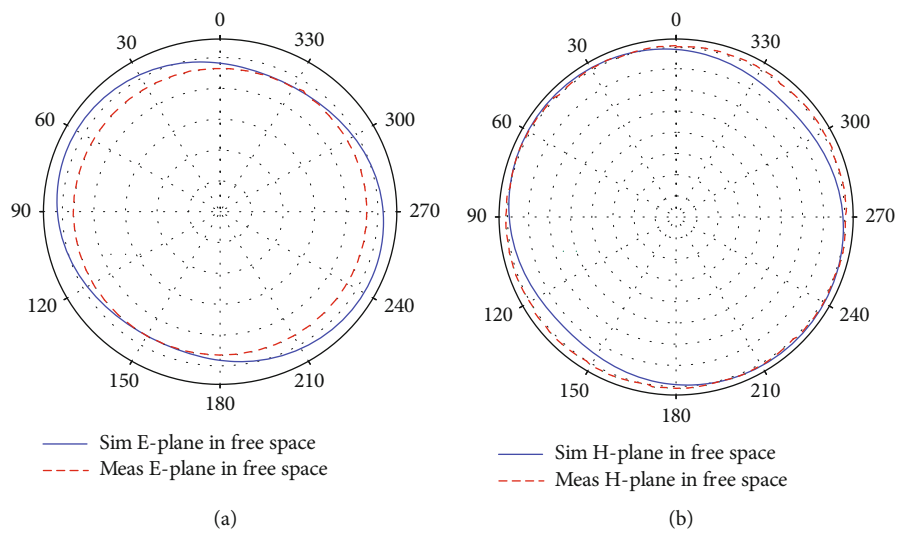

(a)   (b)

FIGURE 9: 2D radiation pattern of the antenna in free space at 915 MHz.

contains distinct layers such as a full ground plane, a low-profile 0.254 mm thick Roger RT5880 substrate ($\varepsilon_r = 2.2$ and $\tan \delta = 0.0009$), and a slotted patch, as shown in Figure 2. The complete volume of the antenna is $7 \times 7 \times 0.254$ mm^3 ($0.08\lambda_g \times 0.08\lambda_g \times 0.003\lambda_g$). The reported antenna is simulated in high-frequency structure simulator (HFSS) software, and the S_{11} of the antenna is found to be -25 dB at the working frequency of 915 MHz and the operating bandwidth of the designed antenna seems to be 21.85%. The optimized values of this antenna are summarized in Table 1.

2.1. Proposed Antenna Design Procedure. The design procedure of the proposed implantable antenna is explained as follows:

(1) In step I (Figure 3(a)), a triangular-shaped slot is introduced on the left side of the patch to generate a frequency band at 1.5 GHz, but return loss is not less than -10 dB as can be seen in Figure 4

(2) Then, in step II (Figure 3(b)), in order to keep the value of the S_{11} (dB) less than -10 dB and to shift the frequency band towards a lower band, a T-shaped slot is introduced in a truncated patch to operate the antenna at 1.4 GHz

(3) Then, in step III (Figure 3(b)), an X-shaped slot is introduced inside the patch. By introducing this slot, it has shifted the band from 1.4 GHz to 0.7 GHz (700 MHz)

(4) Then, in step IV (Figure 3(c)), the proposed novel shape is designed to help to resonate the antenna at the desired frequency at 0.915 GHz

(5) Figure 5 indicates the diagrammatic flow of the proposed antenna to show the entire work procedure

2.2. Parametric Analysis of the Proposed Antenna. The analysis of parameters of the implantable antenna is well explained in this section. The reflection coefficient at 0.915 GHz can be adjusted by varying the values of the important parameters such as length of the patch resonator "S_2," width of the feed patch "S_4," length of the patch slot at 45° angle "S_3," length of the upper left resonator of the patch "S_8," and changing the position of the via as presented in Figure 6. Figure 6(a) illustrates that by selecting the range of value of "S_2" from 2.5 mm to 3.34 mm, the frequency band shifted from 1.6 GHz to 0.915 GHz (685 MHz). When the value of the "S_4" is changed from 0.3 mm to 0.7 mm, then the frequency band shifted from 1.5 GHz to 0.915 GHz (585 MHz) as presented in Figure 6(b). From Figure 6(c), it is also noticed that when the values of the "S_3" are varied from 1.6 mm to 1.8 mm, then the frequency band increases from 0.60 GHz to 0.75 GHz (150 MHz). Again, when the value of "S_8" is varied from 2 mm to 3 mm, then there is a shift in the frequency from 1.7 GHz to 0.9 GHz (800 MHz) as shown in Figure 6(d). By changing the position of the via in the proposed patch antenna, the frequency band shifted higher to our targeted frequency band. It is noticed
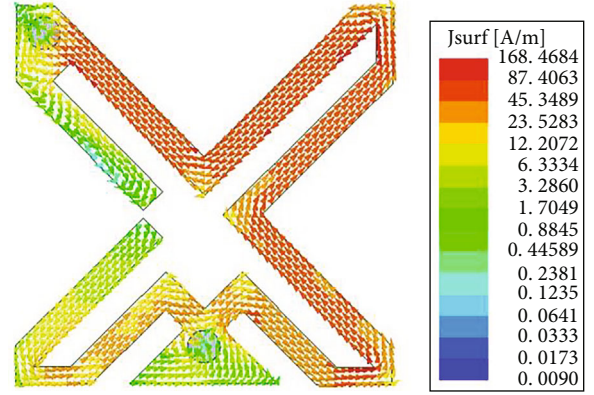

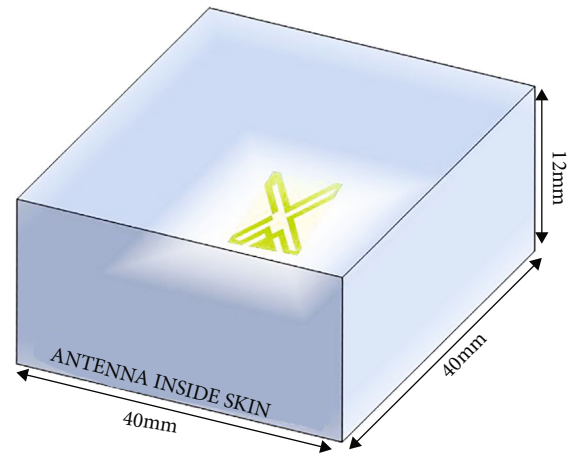FIGURE 10: Current distribution throughout the patch at 915 MHz.

FIGURE 11: Perspective view of the skin phantom box.

from Figure 6(e) that when the via is placed at position 1, then the frequency band was 1.4 GHz, and we got the 0.8 GHz band by changing the via from position 1 to position 2, and finally we achieved our desired frequency band 0.915 GHz by changing the via from position 2 to position 3.

2.3. Equivalent Circuit Modeling. An equivalent circuit model for the proposed implantable antenna is designed using Advanced Design System (ADS) software. Figure 7(a) indicates the circuit model and the impedance matching Smith chart for the proposed antenna system. The circuit model consists of one capacitor, a resistor, and an inductor. Figure 7(b) presents the comparison between the reflection coefficient obtained from the proposed antenna and the proposed circuit model.

3. Results and Discussion

3.1. Antenna in Free Space. The designed biomedical implantable patch antenna is fabricated on a Roger RT5880 substrate with thickness of 0.254 mm and tested inside free space. A vector network analyzer (VNA) is used to measure the S_{11} of the implantable antenna. In the case of the simulated results, the designed antenna covers the
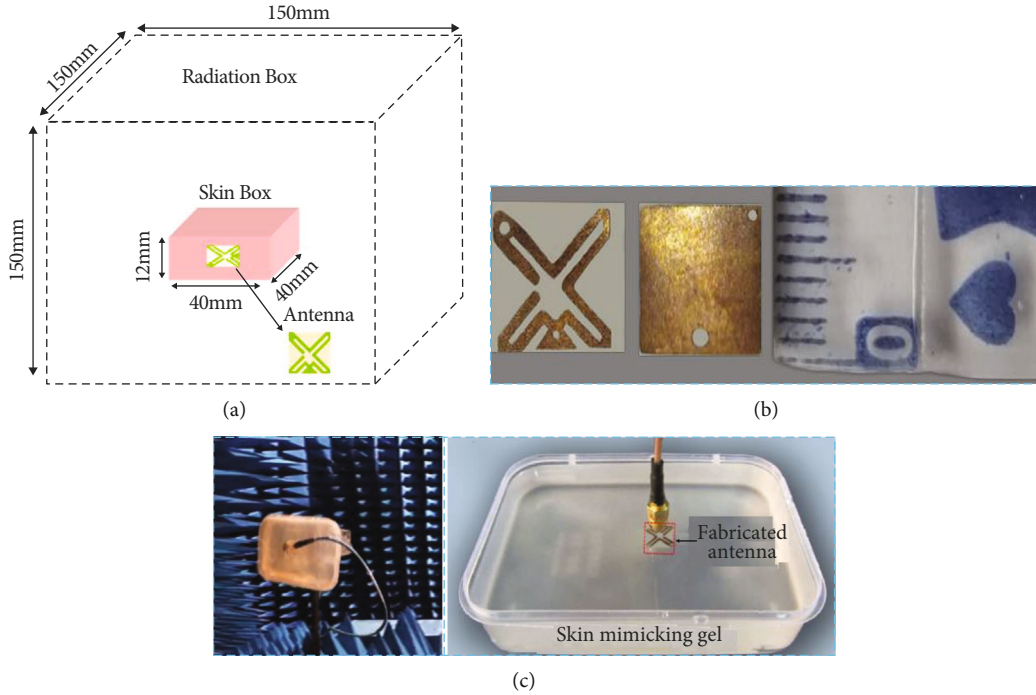
(a)

(b)

(c)

FIGURE 12: Antenna inside the skin of human tissues: (a) perspective view, (b) fabricated prototype of the antenna, and (c) experimental setup to measure the pattern and S_{11}.

bandwidths from 800 MHz to 1000 MHz (200 MHz) at 915 MHz while in the case of the measurements, the antenna covers the bandwidth from 795 MHz to 998 MHz (203 MHz) at 915 MHz as can be seen in Figure 8.

The E- and H-planes of the antenna are simulated and measured in free space (see Figure 9). The two-dimensional (2D) radiation pattern describes the behavior of the antenna. The designed antenna behaves as an omni-directional pattern in both planes at the 915 MHz frequency band. The current density of the implantable antenna is shown in Figure 10. The current mainly flows around the upper- and bottom-sided resonators and feed patch. The red colored arrows indicate that the portion of the antenna has major contribution in operating at the desired frequency band.

3.2. Antenna inside the Skin. To explore the appropriateness of the antenna inside the skin for biomedical telemetry applications, the proposed design is simulated and tested inside skin tissue in this section. Consequently, to design an antenna for the applications in biotelemetry that had high precision, the presence of the human body phantoms must be taken into consideration while calculating SAR. For that, the antenna performance in proximity of human phantoms and the SAR values at 915 MHz are also evaluated. The area of the phantom box is 20×20 mm^2 as can be seen in Figure 11. HFSS Studio is used for simulating the proposed antenna.

In an ideal case, in-body antennas should be planned to avoid the significant coupling effects from the human tissues. While testing the antenna inside the skin of the human body, it is placed 2 mm deep inside the skin tissue
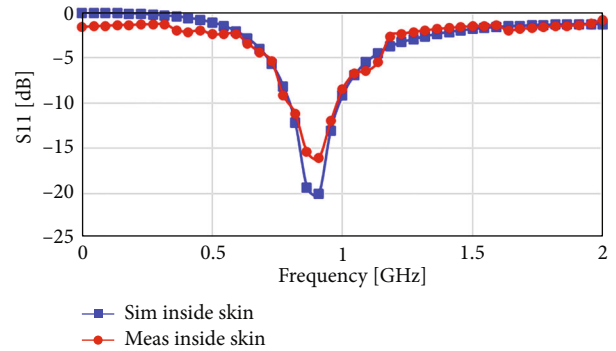

FIGURE 13: Comparison between the simulated and measured S_{11} of the antenna inside skin tissue.

as shown in Figure 12. To estimate these effects, the reported design is kept inside a 40 mm × 40 mm box of skin tissue. A "skin-mimicking gel" with relative permittivity (ε_r) of 43 and electrical conductivity (σ) of 1.40 is used, as its properties are very close to those of human skin tissue.

The contrast between the simulated and measured S_{11} of the antenna inside the skin is described in Figure 13. The simulated S_{11} inside the skin indicates that the bio-medical antenna operates from 780 MHz to 1000 MHz (220 MHz) at 915 MHz while the fabricated antenna inside the mimicking gel, on the other side, featured bandwidths from 785 MHz to 998 MHz (213 MHz). This proves that both simulated and measured results have good agreement among each other.

Figure 14 presents the E- and H-planes of the simulation and measurement results of the radiation pattern inside skin tissue. The 2D radiation pattern describes the behavior of
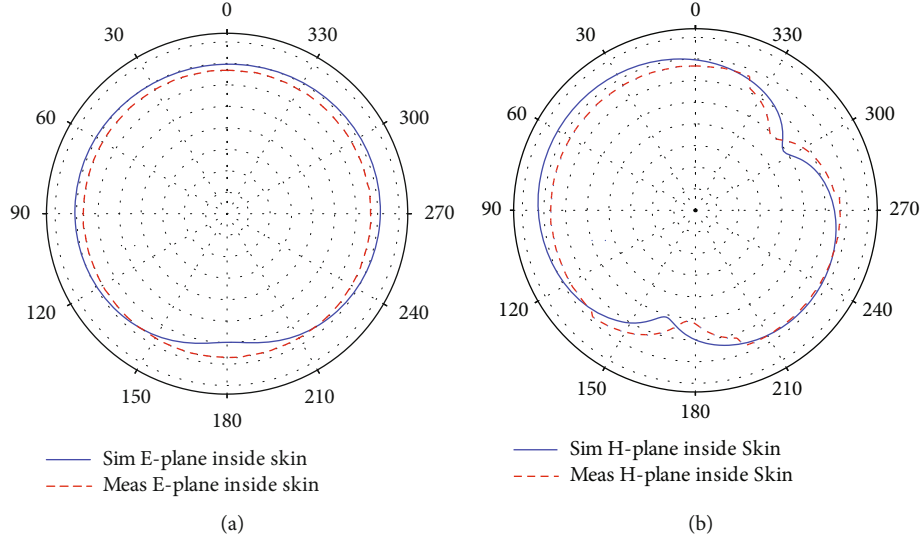
FIGURE 14: Simulated and measured far field results at 915 MHz inside skin tissue.
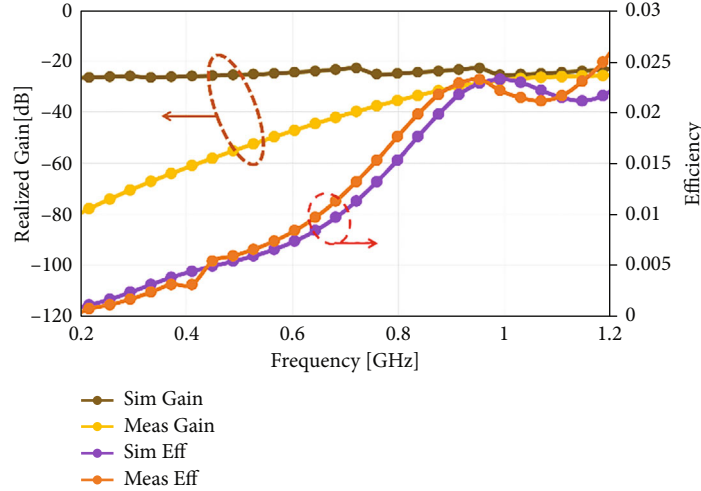

FIGURE 15: Simulated and measured gain and efficiency graph inside the skin.

the antenna inside the skin. These far field results prove that the antenna inside the skin has an omnidirectional radiation pattern in both planes at the 915 MHz frequency band. The simulated realized gain value inside the skin is found to be -22 dB at 915 MHz, whereas measurement results give the realized gain of -28 dB at 915 MHz. The simulated and measured efficiency and gain graph is presented in Figure 15. The presented graph indicates that the antenna has simulated efficiency of 2.2% while the measured efficiency is 2.1% inside the skin.

3.3. Specific Absorption Rate (SAR).
The radiations of electromagnetic waves may cause health risks to the human body, and such risks are calculated in terms of SAR. The relationship between the input power and the SAR is as follows [10]:

$$\text{SAR} = \frac{\sigma \, | E^2 |}{\rho}, \tag{1}$$

where σ and ρ denote the thermal conductivity (S/m) and the mass density (kg/m^3), respectively, while E is the electric field intensity (V/m). The electric power intensity is related to the signal power as follows [13]:

$$\text{Power} \left(\frac{\text{W}}{\text{m2}} \right) = \frac{(E(\text{V/m}))^2}{377}. \tag{2}$$

SAR simulations were accomplished when the proposed antenna is kept inside the skin as well as inside the muscle. Input power pin is kept constant at 0.5 W with the SAR evaluated based on the IEEE/IEC 6270-1 standard, averaged over 1 g of mass tissue. SAR values inside the skin are calculated as 8.17 W/kg at 915 MHz as presented in Figure 16.

3.4. Link Budget Analysis.
The telemetry range between the implanted device and the external base station must be determined in order to successfully communicate biological data. However, the link budget estimates are affected by a
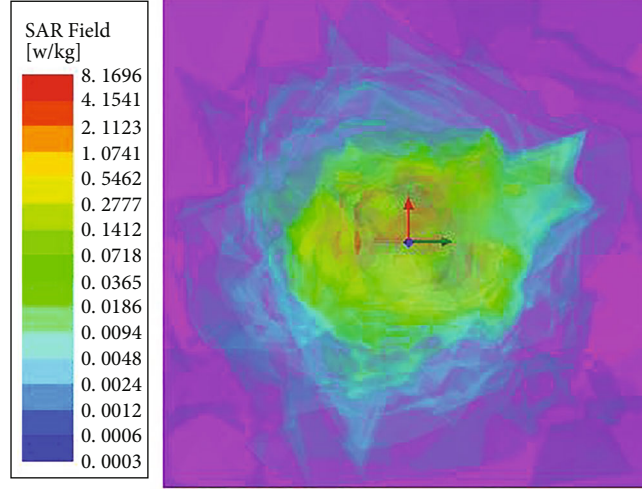
FIGURE 16: SAR distribution of the proposed antenna inside skin tissue over 1 g at 915 MHz.

variety of losses, including free space losses, cable losses, and antenna material and mismatch losses [14]. The link margins were calculated using the Friis equation to calculate the difference between the antenna power (A_P) and the necessary antenna power (R_P), and the link margin should be more than 20 dB for consistent communication. Table 2 lists the important parameters utilized in these computations. The following formula can be used to calculate R_P:

$$R_P = \frac{E_b}{N_o} + KT + B_r. \tag{3}$$

The phase shift keying, Boltzmann's constant, temperature, and bit rate are represented by E_b/N_o, K, T_o, and B_r, respectively. A_P, on the other hand, may be computed as follows:

$$A_P(dB) = P_a + G_a + G_b + L_f. \tag{4}$$

The transmission power, implanted antenna gain, and receiver monopole antenna gain are represented by P_a, G_a, and G_b, respectively. The free space losses are represented by L_f, which may be calculated using the formula below:

$$L(dB) = 20 \log \left(\frac{4\pi d}{\lambda} \right). \tag{5}$$

The distance between the implanted antenna and the external controlling device, which can range from 2 to 30 meters, is denoted by d. For the safety of patients, the European Research Council limits the input power to 25 W and the $EIRP_{max}$ for the ISM (915 MHz) band to 20 dBm [15]. For the ISM (915 MHz) band, the in-body communication range was calculated. The availability of battery power and circuitry are the key problems of the IMDs. The skin implantation is considered depending on the application of the proposed antenna based on the input power. The anticipated transmission power P_t of the proposed antenna is 16 dBm,

TABLE 2: Parameters of the link budget of the stated design.

| Parameters	Variables	Value
Resonance frequency	f_o(MHz)	915
Noise power density	N_o(dB/Hz)	-203.93
Transmitter power	P_{Tx}(dBm)	-4
Polarization mismatch loss	P_L(dB)	1
Temperature	T_o(Kelvin)	273
Free space path loss	L_f(dB)	Distance dependent
Transmitter antenna gain	G_{Tx}(dBi)	Scenario dependent
Receiver antenna gain	G_{Rx}(dBi)	2
Boltzmann constant	K	1.38×10^{-23}
Available power	A_P(db)	Distance dependent
Bit rate	B_r(Mbps)	1
Required power	R_P(dB)	-134.64
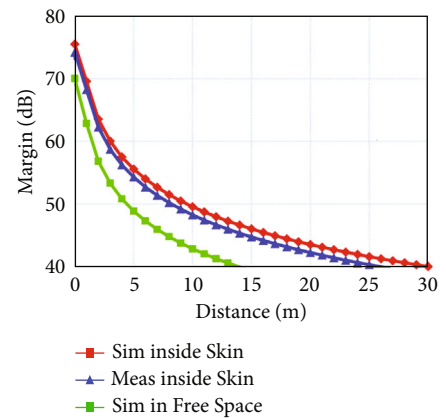
FIGURE 17: SAR distribution of the proposed antenna inside skin tissue over 1 g at 915 MHz.

TABLE 3: Performance comparison of the proposed antenna with recent work.

Ref. no.	Dimensions $(mm^3)/(\lambda_g{}^3)$	Operating frequency (GHz)	Realized gain (dB)	Operating bandwidth (%)	SAR (W/kg) @ 1 g
[8]	$(23 \times 16.4 \times 1.27)/(0.098 \times 0.070 \times 0.005)$	0.402	-34.9	12.9	284.5
[10]	$(25 \times 20 \times 0.07)/(0.34 \times 0.27 \times 0.00095)$	2.45	-16.8	1.22	1.0
[11]	$(15 \times 21.5 \times 1.5748)/(0.39 \times 0.56 \times 0.039)$	2.45	<-15	3.2	Not calculated
[12]	$(3.14 \times 100 \times 2.54)/(0.082 \times 2.6 \times 0.066)$	0.4/2.45	-33.1/-14.55	38.1/17.6	241.5/149.7
[14]	$(14 \times 14 \times 0.5)/(0.365 \times 0.365 \times 0.013)$	2.45	-15.96	18.36	0.494
[16]	$(3.14 \times 28.6 \times 1.34)/(0.082 \times 0.748 \times 0.035)$	0.402/2.45	-41/-21.3	41/27.8	666/676
[17]	$(3.14 \times 23 \times 0.634)/(0.082 \times 0.60 \times 0.016)$	2.45	-20.3	18.3	649
[18]	$11 \times 11 \times 1.27/(0.107 \times 0.107 \times 0.0123)$	0.915	-29	3.8	Not calculated
[19]	$15 \times 15 \times 1.27/(0.14 \times 0.14 \times 0.0123)$	0.915	-27	10.6	517
[20]	$3.14 \times 22.09 \times 1.27/(0.030 \times 0.22 \times 0.0123)$	0.915	-32.8	12.2	778
This work	$7 \times 7 \times 0.254/(0.08 \times 0.08 \times 0.003)$	0.915	-28	21.85	8.1

and the bit rate B_r is 1 Mbps, based on the skin implanted devices. Figure 17 shows the simulated and measured link margin analysis inside skin tissue of the human body. Data at 1 Mbps might be sent across a distance of more than 15 m. It has been discovered that by altering the data rate and gain, the range of data transmission may be altered. Table 3 shows the performance comparison of the proposed work with some of the previously published relevant works.

4. Conclusion

This paper provides a low-profile ISM band compact-size patch antenna for the applications in biomedical implants. The presented antenna is simulated by using HFSS software. This proposed antenna resonates in the ISM band at 915 MHz. The antenna is designed on a Rogers material of RT/Duroid 5880 ($\varepsilon_r = 2.2$, $\tan \delta = 0.0009$) with complete dimensions of 7 mm × 7 mm × 0.254 mm. The measured gain of the antenna inside the skin-mimicking gel is calculated as -28 dB at 915 MHz, while the measured bandwidth of the antenna reported is 21.85% inside the skin-mimicking gel. The SAR values are found to be 8.1 W/kg inside the skin. Problems of compliance with biocompatibility and safety related to the construction of medical applications were also discussed. This antenna is miniaturized and an ideal applicant for in-body biomedical applications.

Data Availability

Data is available on request. The corresponding author can be contacted for any relevant data.

Conflicts of Interest

The authors declare that they have no conflicts of interest.

Acknowledgments

References

[1] M. Yousaf, I. B. Mabrouk, M. Zada et al., "An ultra-miniaturized antenna with ultra-wide bandwidth characteristics for medical implant systems," *IEEE Access*, vol. 9, pp. 40086–40097, 2021.

[2] A. Ghaffar, W. A. Awan, N. Hussain, S. Ahmad, and X. J. Li, "A compact dual-band flexible antenna for applications at 900 and 2450 MHz," *Progress in Electromagnetics Research Letters*, vol. 99, pp. 83–91, 2021.

[3] D. Nguyen and C. Seo, "An ultra-miniaturized antenna using loading circuit method for medical implant applications," *IEEE Access*, vol. 9, pp. 111890–111898, 2021.

[4] M. Yousaf, I. B. Mabrouk, F. Faisal et al., "Compacted conformal implantable antenna with multitasking capabilities for ingestible capsule endoscope," *IEEE Access*, vol. 8, pp. 157617–157627, 2020.

[5] M. S. Singh, J. Ghosh, S. Ghosh, and A. Sarkhel, "Miniaturized dual-antenna system for implantable biotelemetry application," *IEEE Antennas and Wireless Propagation Letters*, vol. 20, no. 8, pp. 1394–1398, 2021.

[6] Z. Xia, H. Li, Z. Lee et al., "A wideband circularly polarized implantable patch antenna for ISM band biomedical applications," *IEEE Transactions on Antennas and Propagation*, vol. 68, no. 3, pp. 2399–2404, 2020.

[7] L. Xu, Y. Bo, W. Lu, L. Zhu, and C. Guo, "Circularly polarized annular ring antenna with wide axial-ratio bandwidth for biomedical applications," *IEEE Access*, vol. 7, pp. 59999–60009, 2019.

[8] R. Li, B. Li, G. Du, X. Sun, and H. Sun, "A compact broadband antenna with dual-resonance for implantable devices," *Micromachines*, vol. 10, no. 1, p. 59, 2019.

[9] K. N. Ketavath, D. Gopi, and S. S. Rani, "In-vitro test of miniaturized CPW-fed implantable conformal patch antenna at ISM band for biomedical applications," *IEEE Access*, vol. 7, pp. 43547–43554, 2019.

[10] K. K. Naik, S. C. Teja, B. V. Sailaja, and P. A. Sri, "Design of flexible parasitic element patch antenna for biomedical application," *Progress in Electromagnetics Research M*, vol. 94, pp. 143–153, 2020.

[11] N. H. Sulaiman, N. A. Samsuri, M. K. A. Rahim, F. C. Seman, and M. Inam, "Compact meander line telemetry antenna for implantable pacemaker applications," *Indonesian Journal of Electrical Engineering and Computer Science*, vol. 10, no. 3, p. 883, 2018.

[12] P. Loktongbam, D. Pal, and C. Koley, "Design of an implantable antenna for biotelemetry applications," *Microsystem Technology*, vol. 26, pp. 2217–2226, 2020.

[13] N. Ganeshwaran, J. K. Jeyaprakash, M. G. N. Alsath, and V. Sathyanarayanan, "Design of a dual-band circular implantable antenna for biomedical applications," *IEEE Antennas and Wireless Propagation Letters*, vol. 19, no. 1, pp. 119–123, 2020.

[14] W. Lei, H. Chu, and Y. Guo, "Design of a circularly polarized ground radiation antenna for biomedical applications," *IEEE Transactions on Antennas and Propagation*, vol. 64, no. 6, pp. 2535–2540, 2016.

[15] V. K. Gupta and D. Thakur, "Design and performance analysis of aCPW-fed circularly polarized implantable antenna for 2.45 GHz ISM band," *Microwave and Optical Technology Letters*, vol. 62, no. 12, pp. 3952–3959, 2020.

[16] S. Shekhawat, S. V. Gunaram, and D. Bhatnagar, "CPW fed implantable elliptical patch antenna for biomedical application," *AIP Conference Proceedings*, vol. 2220, article 130068, 2020.

[17] L. Luo, B. Hu, J. Wu, T. Yan, and L.-J. Xu, "Compact dual-band antenna with slotted ground for implantable applications," *Microwave and Optical Technology Letters*, vol. 61, no. 5, pp. 1314–1319, 2019.

[18] L. Xu, J. Xu, Z. Chu, S. Liu, and X. Zhu, "Circularly polarized implantable antenna with improved impedance matching," *IEEE Antennas and Wireless Propagation Letters*, vol. 19, no. 5, pp. 876–880, 2020.

[19] C. Liu, Y. Zhang, and X. Liu, "Circularly polarized implantable antenna for 915 MHz ISM-band far-field wireless power transmission," *IEEE Antennas and Wireless Propagation Letters*, vol. 17, no. 3, pp. 373–376, 2018.

[20] K. Zhang, C. Liu, X. Liu, H. Guo, and X. Yang, "Miniaturized circularly polarized implantable antenna for ISM-band biomedical devices," *International Journal of Antennas and Propagation*, vol. 2017, 9 pages, 2017.

[21] Y. Zhang, C. Liu, X. Liu, K. Zhang, and X. Yang, "A wideband circularly polarized implantable antenna for 915 MHz ISM-band biotelemetry devices," *IEEE Antennas and Wireless Propagation Letters*, vol. 17, no. 8, pp. 1473–1477, 2018.